Enriched Encephalon Tumor Segmentation using Tessellation Automata with High Performed Levelset using Radiosurgery Applications

Kamalam. N[1], Muthumari. A[2]

[1,2]Department of Computer Science & Engineering, University College of Engineering
Nagercoil, Tamil Nadu, India
kamalam.cse@gmail.com
muthu_ru@yahoo.com

Abstract: ***Segmentation of brain tissues is gaining popularity with the advance of image guided surgical approaches. This work proposes a fast and robust practical tool for segmentation of solid tumors in radiosurgery application. For this, a cellular automata (CA) i.e. Tessellation Structure based seeded tumor segmentation method is used on MR images, which standardizes the volume of interest and seed selection. The procedure starts by establishing the connection of CA based segmentation to the graph theoretic methods to show that iterative CA framework solves the shortest path problem by modifying the state transition function from the CA. A sensitive parameter is introduced to adapt the heterogeneous tumor segmentation problem. Then a smoothness constraint using level set active surfaces is imposed by an EM algorithm over a probability map constructed from CA State. A standard EM level-set propagates normal to its boundary uniformly at a constant speed which will stop on the desired boundary. Finally a CA algorithm is introduced to differentiate necrotic and enhancing tumor tissue with different grade is obtained by a Fuzzy c-means clustering technique to categorize the various type of affected cells content for detailed assessment of radiation therapy response.***

Keywords: Encephalon tumor segmentation, radiotherapy, Tessellation automata, Fuzzy clustering, magnetic resonance imaging (MRI

1. Introduction

1.1 Motivation and Overview

Motivated by surveillance applications in clinical field, the fuzzy diagnosis concept is widely applied. The advent of MRI scanning protocols has allowed accurate follow-up of tumor growth through volumetric measurements. Fuzzy can range between the supervised classification of a number of clinical cases within different classes of pathologies, through a set of rules concerning both linguistic and numerical data, and the unsupervised segmentation of medical images through data based methods of analysis concerning spatially distributed numerical variables. Image segmentation is one of the most important precursors for image processing based applications and has a decisive impact on the overall performance of the developed system. Robust image segmentation has been the subject for research for many years but the published research indicated that most of the developed image segmentation algorithms have been designed in conjunction with the particular applications. The segmentation process consists of separating a digital image into several disjoint regions, whose characteristics such as intensity, color and texture. Outlining the brain tumor contour is a major step in planning spatially localized Radiotherapy (e.g., Cyber knife, iMRT) which is usually done manually on contrast enhancedT1-weighted magnetic resonance images (MRI) in current clinical practice. On T1 MR Images acquired after administration of a contrast agent (gadolinium) blood vessels and parts of the tumor, where the contrast can pass the blood-brain barrier are observed as hyper intense areas. There are various attempts for brain tumor segmentation in the literature which use a single modality, combine multi modalities and use priors obtained from population atlases [4]. Interpretation of the radiological evolution of the tumor appears of utmost importance for therapeutic management, for the evolution of different grades of tumor cells which is an aggressive brain tumor with poor outcome. With the outcome of patients with primary brain tumors, we analyzed the three most common tumor affected cells: glioblastoma (GBM or grade 4 glioma, 184 or 49%) astrocytoma (grade 2 or 3 glioma, 100 or 26%) and meningioma (42 or 11%). Glioblastoma multiforme (GBM), is a primary malignant brain tumor, is the most common form of the glioma tumors which in spite of multimodality treatments, remains as an incurable and rapidly fatal disease. The anatomic location of a glioma influences prognosis and treatment options. A few studies aim at discovery of the distribution of gliomas in different anatomic areas of the brain. By using Clustering technique we are going to categorize the various grade levels of tumor affected cells and the necrotic region. By using this technique the therapeutic can diagnosis the type of cell damaging and locating the cells which are cancerous or non-cancerous cell.

Segmentation of actual growth, registration on a virtual brain atlas, and identification of model parameters corresponding to optimal matching between actual and simulated evolution. Modalities which give relevant information on tumor and edema/infiltration such as Perfusion Imaging, Diffusion Imaging, or Spectroscopic Imaging provide lower resolution images compared to T1 or T2 weighted sequences, and the former are generally not preferable for geometric measurements. The approach presented herein aims at providing a more generic and robust for the segmentation of blobby- shaped tumor structures with high performed level set and it gives the various different level of damaged cells and the death cells. The popular trend in the area, as in the aforementioned approaches, is to attempts to develop better algorithms from the image processing perspective

that work on a particular MRI protocol continue in parallel not only to obtain proper information from each channel to be combined, but also due to the practical need to routinely quantify tumors in a clinical environment [6]. In general, these region-based models are widely used in image segmentation [10] it several advantages over gradient-based techniques for segmentation, including greater robustness to noise. However, classical active contours had the problem of being "only as good as their initialization," even when using level-set surfaces in 3D. Because the tumor class does not have a strong spatial prior, many small structures, mainly blood vessels, are classified as tumor as they also enhance with contrast. Ho et al. used fuzzy classification of pre- and post-contrast T1 images to obtain a tumor probability map to evolve a level-set surface [11]. Liu et al. have adapted the fuzzy connectedness framework for tumor segmentation by constructing a rectangular volume of interest selected through identifying the first and last slice of the tumor and specifying a set of voxels in the tumor region [6]. A standard level-set propagates normal to its boundary uniformly at a constant speed α. Our region competition-based model modulates this propagation term using image forces to change the direction of propagation, so that it shrinks when the boundary encloses parts of the background (B), and grows when the boundary is inside the tumor region (A).

Interactive algorithms have become popular for image segmentation problem in recent years. Graph based seeded segmentation framework has been generalized such that graph-cuts(GC)[12],random walker (RW) [13],Shortest paths and power watersheds [14] have been interpreted as special cases of a general seeded segmentation algorithm, which solves a minimization problem involving a graph's edge weights constrained by adjacent vertex variables or probabilities. In [15], the connection between GC, RW and shortest paths was shown to depend on different norms: (GC); (RW); (SP) in the energy that is optimized. Geodesic distance between foreground and background seeds were also incorporated into other shortest path based segmentation algorithms by [16] and [17]. Although it was reported that the shortest paths and RW produce relatively more seed dependent results, it can be argued that the global minimum of an image segmentation energy is worth as good as the ability of its energy to capture underlying statistics of images [18], and a local minimum may produce a solution closer to the ground truth than that of a global minimum. Hence, with good prior information provide as in the case of a seeded image segmentation problem, effectively finding a good local minima becomes meaningful and worthwhile.

In order to improve the efficiency of this task, we have studied different clustering algorithms. We made several experiments with a number of fuzzy approaches to clustering for medical image segmentation. These methods seem to adaptively perform an efficient unsupervised clustering, not affected by the dimensionality of the feature space. Moreover, fuzzy clustering methods produce a voxel classification, related to the membership function of clusters, and can add some kind of smoothness to voxel classification. This helps to better define surfaces of the anatomical objects described by segmentation. Comparatively for K-Means clustering the degree of membership for a pattern in a particular cluster is 1 if the pattern belongs to the cluster or 0 if it doesn't. In fuzzy set theory, a pattern can belong to 2 or more Clusters simultaneously where the membership grades determine the degree to which the pattern belongs to these clusters. Tessellations Automata is a cellular automaton consists of a regular grid of cells each in one of a finite number of states. CA algorithm to establish the connection of the CA based segmentation to the graph theoretic methods to show that the iterative CA framework solves the shortest path problem with a problem proper choice of the transition rule. Level set offer significant advantages over conventional statistical classification and mathematical morphology, however with constant propagation need careful initialization and can leak through weak or missing boundary parts. A smoothness constraint using level set active surfaces is imposed over a probability map constructed from resulting CA states.

This study is used for T1 and T2 weighted images to develop a method based on the fuzzy-c-mean clustering to extract the meningioma, astrocytes and glioma type cells from the MR image. The overall aim was to successfully complete tumor image segmentation with high performed level set, and at the same time, to effectively detect the various grades of tumor.

2. Method

In this section, the complete segmentation framework to segment tumors and clustering of cell are enclosed is presented in detail. An overview of the algorithm with the implementation is given in Section II-A. Major steps of the algorithm are explained in detail in Sections II-B, II-C, II-D, and II-E followed by the datasets and methods used for performance evaluation in Section II-F.

2.1 Seed Selection

Our seed selection algorithm employs the same idea to follow the familiar clinical routine to which the clinicians are used to: the volume of interest (VOI), the tumor seeds and the background seeds are determined by using the line already drawn by the user to measure the longest diameter of the tumor. Afterwards, the VOI and the seeds are computed as follows: 1) The line is cropped by 15% from each end and thickened to three pixels wide to obtain tumor seeds; 2) VOI is selected as the bounding box of the sphere having a diameter 35% longer than the line; 3) One-voxel-wide border of this VOI is used as background seeds [see fig 5 and fig 6]

Since the VOI is completely bounded by the background seeds, each path connecting inside and outside the VOI is blocked by a seed. Then, the result of labeling using only the data inside the region is equivalent to using the whole volume whereas the computation time is significantly reduced. In the tumor segmentation application, the cells or nodes in cellular automata framework correspond to the MRI volume voxels in 3-D. A 26 cell cubic neighborhood is used in 3D. MRI intensities

are used as image features. The automata is initialized with user supplied
Tumor and background seeds as explained in Section II-B and iterated by the following rule:

$l^{t+1}_i = l^t_{i*}$ and $x_i^{t+1} = g(i,i^*)x^t_{i^*}$ where $i^* = \text{argmax}_{j \in Ni}\ g(i,j)x_j^t$

where is a pixel similarity or transition function bounded to [0, 1], which is equivalent to the edge weight function w_{ij} in the seeded segmentation framework. A typical symmetric edge weight function depending on the image features, is given by the absolute intensity difference or gradient magnitude between neighboring nodes i and j.

$$g(i , j) = e^{-||Ii - Ij||}$$

where I_i denotes the MR image intensity at node i. In the seeded tumor segmentation application over contrast enhanced T1-weighted MRI for heterogeneous tumors, which mostly consist of a ring enhancing region around a dark necrotic core(and also irregular border), most of the foreground seeds fall in the necrotic region. This sometimes causes the segmentation algorithm to get stuck at necrotic to enhancing tumor transition borders. To overcome such problems, prior knowledge that tumor voxels are brighter in post contrast T1-MRI can be utilized. This is can achieved by modifying the transition function g(i,j) by inserting a spatially varying parameter

$$g(i,j) = \begin{cases} e^{-\beta||Ii-Ij||}, & I_i > I_j \text{ and } I_j = \text{Tumor} \\ e^{-\beta||Ii-Ij||}, & \text{otherwise} \end{cases}$$

The intuition here is based on the observation that the enhancing tumor cells are brighter than the normal tissue, and more centrally located necrotic core is darker. Therefore, by adjusting the parameter, the weight reduction (i.e., the strength loss) of a tumor state while passing through a ramp up gradient is adjusted to be lower than other cases.

The effect of parameter on the segmentation performance in terms of Dice overlap measure is demonstrated in. Although, some of the properties we derived for the algorithm are no more valid, as due to asymmetric edge weight values, we can no longer interpret the algorithm in the undirected graph framework our experimental results revealed that the new tumor CA (tca) revealed that the new tumor CA (tCA) algorithm significantly improved the results obtained, especially on glioblastomas [27]. Tumor and background seeds as explained in Section II-B and iterated by the following rule.

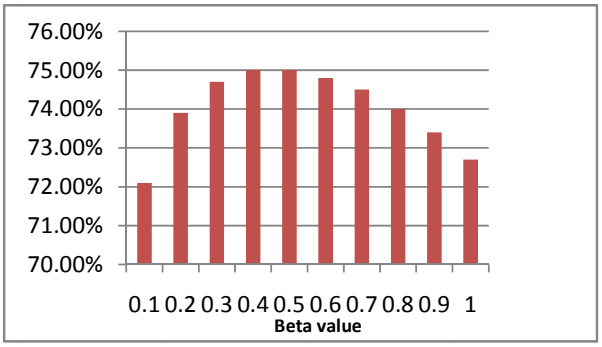

Figure 1. Effect of β on the Segmentation of Performance

2.2 CA Algorithm

Steps of the proposed cellular automata based tumor segmentation algorithm is shown in Fig. 5. First, (a) the user draws a line over the largest visible diameter of the tumor; (b) using this line, a VOI is selected with foreground and background seeds; Fig 6 (a,b)-(c) and Fig 7 CA algorithm is run on the VOI for each two sets of seeds (for the foreground and background) to obtain strength maps for background(a) and foreground (b) at each voxel two strength maps are combined to obtain the tumor probability map ; Fig 8 a level set surface is initialized at and the map is used to evolve the surface which converges to the final segmentation map obtained.

A pseudo code of the Cellular Automata algorithm is given below:

for $\forall l \Leftarrow$ { Tumor , Background}
// Initialize
for $\forall p \in P$
if p is a seed of class l, $x^0_{l,p} = 1$, else $x^0_{l,p} = 0$
end for
Do until convergence
// For each cell…
for $\forall p \in P$
//Neighbors tries to attack current cell
for $\forall q \in N(p)$
Find q*:q with maximum $g(p,q).x^t_{l,q}$
$x^{t+1}_{l,p} = g(p,q^*).x^t_{l,q^*}$
end for
//Copy previous state
$x^t_{l,p} = x^{t+1}_{l,p}$
end for
end do
end for
// Combine strengths for tumor and background to obtain tumor probability map

$$P_T = \ln(x_{Bg}) / \ln(x_{Bg}) + \ln(x_T))$$

//Evolve the tumor surface via a level set embedding

$$\partial s/\partial t = (u-v)(u+v-2PT)N$$

//where u,v are the means inside and outside the surface, and N is the unit normal vector surface S.

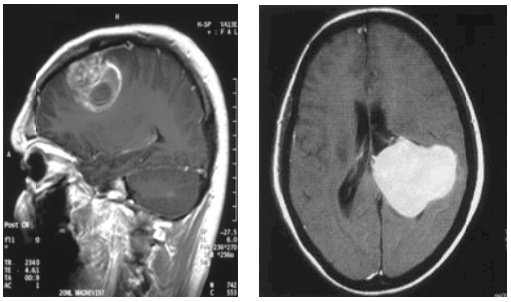

Figure 2.Tumor affected T1MRI image

2.3 EMD based Level set Evolution

Let {p1; . . . ; p_N} and {q_1; . . . ; q_N} be the two histograms, where we name the bins as 1; 2; . . .; N.

In this paper, all histograms are Normalized (sum up to unity). Assume that the cost of moving a unit of probability mass from bin i to bin j is c_{ij} ($c_{ii} = 0$). The idea behind the EMD [29] is to find the cheapest way to transfer the probability mass from $\{p_1; \ldots ; p_N\}$ to $\{q_1; \ldots ; q_N\}$. The cost of this cheapest possible transfer measures the distance between the two histograms. Let us now limit ourselves to cases in which the histograms are one-dimensional. In this case, there is a unique "path" from every bin i to every bin j and it necessarily passes through other bins in between. The unique path between every two bins significantly constrains the possible flows and leads to the following:

Claim: Let $P = \{p_1; \ldots ; p_N\}$ and $Q = \{q_1; \ldots ; q_N\}$ be discrete probability distributions on N bins. Let $\{P1; \ldots ; P_N = 1\}$ and $\{Q_1; \ldots ; QN = 1\}$ be the corresponding cumulative distribution functions (CDFs): $P_{i=} p_1 + \ldots + p_i$; $Q_{i=} q_1 + \ldots + qi$.

Assume that the cost structure is $c_{ij} = |i - j|$. Then,

$$EMD(P,Q) = \Sigma^{N}_{i=1} |P_i - Q_i|$$

Proof. First suppose that $P_1 \geq Q_1$; $P_2 \geq Q_2$; $\ldots$; $P_N = Q_N = 1$. The first bin currently contains p1 mass, and needs to contain $q_1 \leq p_1$ mass. Therefore, we have to move $p_1 - q_1$ mass out, necessarily to bin 2. Now, we have $p_2 + p_1 - q_1$ mass in bin 2. We need leave there only q_2 mass. By the assumption $P_2 \geq Q_2$, we have $p_2 + p_1 - q_1 \geq q_2$ so we have to move $p_2 + p_1 - q_1 - q_2 = P_2 - Q_2$ mass out of this bin, necessarily to bin 3.

Note that the cost for the mass moving we have done so far is $|P_1 - Q_1| + |P_2 - Q_2|$. We continue this way and obtain, in this specific case, that the only feasible flow that transforms $\{p_1; \ldots ; p_N\}$ to $\{q_1; \ldots ; q_N\}$ indeed costs $\sum_i |P_i - Qi|$. Thus we have proven the claim for the case where the two CDFs do not intersect—i.e., one CDF is always greater or equal to the other CDF. In the general case where the CDFs intersect, we apply the same argument over each of the segments where one CDF is larger than the other.

Note that our proof relies on the specific cost structure that we chose. Also note that the standard Kolmogorov-Smirnov statistic is defined by $KS(P,Q) = \max_i |P_i - Q_i|$. The claim we proved shows that the EMD

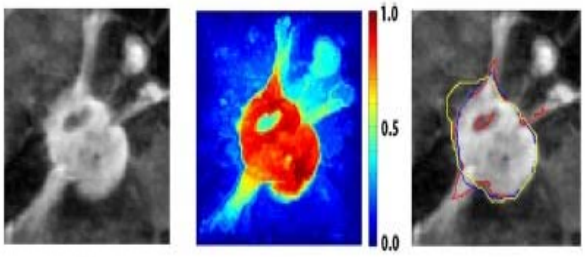

(a) (b) (c)

Figure 3. Effect of Smoothing. a) Tumor image obtained by CA algorithm b)Segmentation result c) before smoothing (red) after smoothing(blue) and expert (yellow)

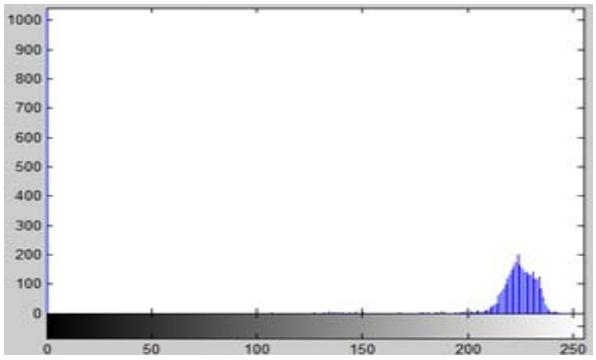

Figure 4. Histogram for Encephalon Tumor image

distance replaces the $L\infty$ norm between the CDFs by the L1 norm. When the surface evolution converges, the final tumor segmentation map is obtained. In Fig 8 the level-set based smoothing over the constructed tumor probability map in (6) constitutes an important part of the proposed method, as the clinical expert segmentation, particularly in radiation oncology, mainly outlines the tumor borders using contouring for radiotherapy planning as opposed to pixel by pixel labeling of the tumor carried out in some validation studies. As a result, our interactive tumor segmentation includes an appropriate intelligent Smoothing of the tumor borders based on the labeling results obtained from this approach. The qualitative effect of adding the smoothing step over the CA result is shown in Fig.3 which exemplifies how the borders are smoothed after level set evolution over the tumor probability map displayed.

2.4 High Grade to Necrotic Clustering

One of the most popular and widely studied clustering algorithms to separate the input data is Fuzzy-c-mean clustering.. By using this algorithm we can get an three level of astrocytomas ,GBM and meningioma type of tumor affected cell affected Based on the differences in gray levels of T1- and T2- weighted images, a two-dimensional intensity histogram, as shown in Figure 1, was created to represent the distribution of intensities in T1 and T2 images. For a pair of 8-bit images, the histogram consisted of a set of 256 × 256 bins, which counted the number of pixels

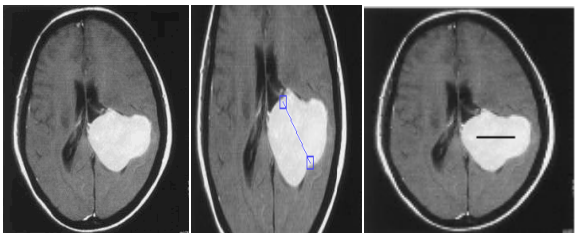

a) b) c)

Figure 5. a) MRI image b) Rough diameter drawn by user c) User Interaction which get Computerized

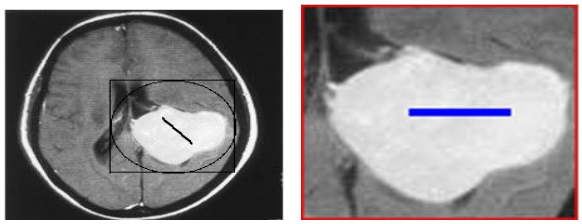

a) b)

Figure 6. Seed Selection Process, a) VOI is selected as the bounding box of the sphere b) Selection of Tumor seed (blue) and background seed as (red)

falling in the given area of the (T1 intensity, T2 intensity) plane. FCM cluster algorithm was used to partition the two-dimensional histogram. Fuzzy C-Means tends to minimize the following objective function:

$$J = \sum_{j=1}^{c} \sum_{i=1}^{n} (U_{ij})^m \, ||x_i^{(j)} - c_j||^2$$

where u_{ij} are the membership values that form the membership matrix U (represents the degree of membership to the C clusters and it has a value in the range of [0 1] for each feature vector x_i to the fuzzy cluster c_j. The parameter m is the called the fuzzifier factor and determines the level of cluster fuzziness. A large value for m results in smaller membership u_{ij} and hence fuzzier clusters.

Steps of the Fuzzy C-Means Clustering Algorithm

1. Consider a set of n data points(vectors) to be clustered.
2. Assume the number of clusters C is known C [2,n].
3. Choose an appropriate level of cluster fuzziness m R, m>1.
4. Initialize the (n x c) size membership matrix U to random variable value such that:

   $U_{ij} \in [0\ 1]$ and $\sum_{j=1}^{c} u_{ij} = 1$
5. Calculate the cluster centers cj using

   $C_j = \sum_{i=1}^{n} (u_{ij})^m x_i \Big/ \sum_{i=1}^{n} (u_{ij})^m$, for j=1…C
6. Calculate the distance measures $d_{ij}=||x_i^{(j)}-c_j||$ for all clusters j=1…C and data points i=1…n.
7. Update the fuzzy membership matrix U according to

   d_{ij}. If $d_{ij}>0$ then $u_{ij} = \left[\sum_{k=1}^{c} (d_{ij}/d_{ik})^{2/m-1}\right]^{-1}$

   If $d_{ij}=0$ then the data point x_j coincides with the cluster center c_j and so full membership can be set $u_{ij}=1$.
8. Loop from step 5 until the change in U is less than a given tolerance.

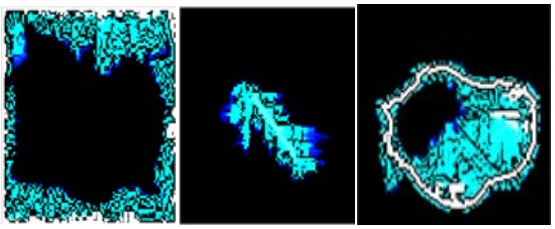

a) b) c)

Figure 7. CA algorithm , a) Applied on Background seed b)Applied on Tumor seed c) Tumor seed selection

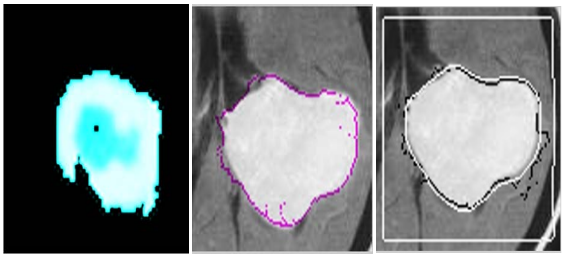

a) b) c)

Figure 8. a) Segmented image b)outline given by CA algorithm c) before EMD (black), after EMD (white)

The objective of the Fuzzy C-Means algorithm is the minimization of the intra-cluster variability. Fuzzy C-Means shares the same problems as K-Means algorithm, namely the initial selection of the cluster centers and the initial choice of weights u_{ij}. The advantages consists in the idea that fuzzy
clustering allows overlapping clusters with partial membership of individual clusters and we can control the level of cluster fuzziness. Because there is no total commitment of a given point to a given cluster, fuzzy clustering algorithms require more memory and are computationally expensive when applied to large datasets.

Necrotic class naturally arises in segmentation using multiprotocol (T1, CE-T1, T2, DWI, etc.) intensity classifiers due to its different intensity characteristics in different modalities. However, our aim in this study is to quantify the necrotic and enhanced parts of the tumor using solely contrast enhanced T1 weighted MRI volumes. This can be achieved by a two step sequential algorithm. Firstly, tumor volume (including both enhanced and necrotic tissues) is segmented by the method as described and then the necrotic and enhanced classes are separated inside the whole tumor volume with the three grade levels.

In CE-T1 MR images, necrotic parts of the tumor are observed as hypo-intense for there is no blood flow into these regions where enhanced parts are hyper-intense. Without any prior information, segmentation using an intensity threshold can be applied by assigning necrotic label to the voxels lower than the chosen threshold and enhanced label to those that are higher. To choose the threshold, we explored using expectation maximization [33] and Otsu's methods [34]. However, usually the two classes are not separable on the intensity histogram even though they could be separated easily on the image as seen on the sample cases.

2.5 Data and Evaluation Methods

Validation studies of the developed method are carried out over four different datasets of all contrast enhanced T1-MR images. The level-set procedure was successfully run on several tumor datasets, and with Clustering techniques. The output of each segmentation is a binary image on the same voxel grid as the original MRI. The image segmentation validation framework to examine various metrics of agreement of segmentation. The Brain Tumor datasets obtained from the Indian MRI Scan and from clinical Radiation center. Here thereby we collected above 42 dataset affected due to various tumor cells. In

radio surgery planning of brain tumors, target tumor volume, which is desired to receive sufficiently high dose, is outlined on MR images by a radio-oncology specialist. As the ground truth for segmentation, we used the tumor contours outlined manually by a radio-oncologist for radio surgery planning. In assessment of the tumor segmentation performance, for each of the tumor cases mean, median, and maximum of the surface distances are calculated using the minimum distances from the sampled points on the algorithm segmentation surface to the manual segmentation surface.

The results of the Cellular automata algorithm is compared to that of the Graph- cut algorithms , Which includes in comparison for its popularity among graph based Segmentation methods and Grow cut is chosen since it is the first algorithm that uses CA for image segmentation. For each of the tumor cases, Graph-cut, Grow-cut and Cellular automata algorithm are run with identical initialization.

3. Result and Discussion

The performance measures, Dice overlap, mean, median, and maximum surface distances and the volume percent error between the ground truth segmentation and the result of the algorithm are reported for the synthetic dataset. The active surface propagation over the constructed probability map aims at correction and improvement of the segmentation by smoothing out the tumor borders, and avoiding sharp protrusions, however, here due to the low intensity contrast between the tumor tissue and the gray matter, the Tumor-cut performed worse than expected.

The clinical classification of tumors along with the different segmentation performance criteria of the CA algorithm over the clinical radio-oncology dataset is tabulated in Table I. The Otsu method is 75.8% on the average whereas the Single threshold produces the average of 80.06 % and the proposed method produces an average of 80.53%. The Dice overlap comparison results among the Graph-cuts, Grow-cut, and the proposed Tumor-cut method. The results we observed with the Graph-cuts approach exhibits similar problems reported before in [14] such as shrinking bias due to minimum cut optimization. The shortest path algorithms, e.g., CA-based methods, showed lack of the shrinking bias problem. The proposed cellular automata algorithm exhibits a lower coefficient of variation (std/mean) on the average compared to the other methods used in validation.

I present 3D qualitative segmentation results from the clinical dataset on sample 2D slices in Fig.10. The mixed necrotic and various types of tumor tissue content as well as non damaged cells are observed. These challenging Scenarios these challenging scenarios exemplify the difficulty level in the segmentation problem, for whose solution interactive algorithms are regarded by the physicians as more feasible than fully-automated ones. The level of interaction in the proposed tumor segmentation algorithm is minimal given by a single line along a 2D axial major diameter of the given tumor. A simple initialization that lasts only 1-2 s for the Encephalon Tumor CA algorithm, lead to reasonably well tumor delineations, which are of important value in quantification of the volume change, as well as necrotic and enhancing tumor tissue content change between a baseline and follow-up study in the clinics for assessment of radiotherapy response. I present the results of the necrotic tissue segmentation and the various grade level of tumor in the subsection.

In Fig 8. I presented a CA based method for labeling necrotic and enhancing tumor tissues content with various grade levels using Earth movers' algorithm for the Enriched and smoothened level set approach. I use a nonparametric local representation of the regions by considering multiple one-dimensional histograms of normalized spatiotemporal derivatives. I Compared with Gaussian kernel in which the smoothened edges are not accurately locate it up. In Earth movers distance metrics we employ a tractable expression for calculating EMD between one-dimensional distributions. A smoothness constraint using level set active surfaces is imposed by an EM algorithm over a probability map constructed from CA State. A standard EM level-set propagates normal to its boundary uniformly at a constant speed which will stop on the desired boundary. The EMD is based on a solution to the transportation problem from linear optimization, for which efficient algorithms are available, and also allows naturally for partial matching. It is more robust than histogram matching techniques, in that it can operate on variable-length representations of the distributions that avoid quantization and other binning problems typical of histograms. It allows for partial matches, and it can be applied to variable-length representations of distributions. Lower bounds are readily available for it, and it can be computed efficiently. The efficient and simple form of EMD, together with the use of the integral histogram, allow the segmentation process to run in real-time, which is extremely important in the medical application. Finally, it would be interesting to apply the earth mover's distance to other vision problems such as classification and recognition based on other types of visual cues. In addition, we surmise that the EMD may be a useful metric also for problems outside the realm of computer vision.

After resulting an enriched segmented image we are going to segment an necrotic part and the other enhancing tissues like meningioma, astrocytes and glioma type cells from the MR image by an Fuzzy C- means

Table 1. Results on mri images by the proposed method encephalon tumor

Tumor ID	*Expectation Maximization (%)*	*Otsu's Method (%)*	*Max. with Single Threshold (%)*	*Proposed CA Method (%)*
Tumorbig.bmp	82.0	82.4	82.5	82.81
Tumor1.bmp	73.7	80.0	83.8	83.54
Tumor2.bmp	84.9	84.5	87.9	88.38
Tumor3.bmp	74.6	87.5	89.0	90.14
Necrotic.bmp	42.5	44.6	57.1	57.8
AVERAGE	71.54	75.8	80.06	80.53

clustering. Clustering of numerical data forms the basis of many classification and system modeling algorithms. The purpose of clustering is to identify natural groupings of data from a large data set to produce a concise representation of a system's behavior. The fuzzy c means clustering method with thresholding is the combination of fuzzy algorithm, c means clustering and thresholding algorithm. In this paper we propose fuzzy c-means clustering method with threshold- -ding for tumor affected cell based image segmentation The goal of a clustering analysis is to divide a given set of data or objects into a cluster, which represents subsets or a group. The partition should have two properties. Homogeneity inside clusters the data, which belongs to one cluster, should be as similar as possible. Heterogeneity between the clusters: the data, which belongs to different clusters, should be as different as possible. The membership functions do not reflect the actual data distribution in the input and the output spaces. They may not be suitable for fuzzy pattern recognition. To build membership functions from the data available, a clustering technique may be used to partition the data, and then produce membership functions from the resulting clustering. Even though it is important for the clinicians to have the capacity to quantify the change in the necrotic content of the tumor after radiation therapy, this differentiation within tumor content is not typically carried out in the clinical routine.

4. Conclusion

I have applied the method to five real datasets, representing different tumor shapes locations, sizes, image intensity, and enhancement. The model allows for different tumor boundaries in each channel, reflecting difference in tumor appearance across modalities. I derive an estimation algorithm and demonstrate superior performance over standard multivariate segmentation on tumor affected cells. A pre- vs. post-contrast difference image is used to calculate probabilities for background and tumor regions by using an CA algorithm. The user interaction time is just a few seconds and typical computation times vary between 1 s to 16 min (on a 3.17 GHz dual processor workstation) depending on the volume of the tumor which ranges between 0.5 and 32 cc. Due to inherent parallelity of the proposed algorithm, computation time can be significantly reduced. The level-set procedure was successfully run on several tumor datasets, and compared with hand

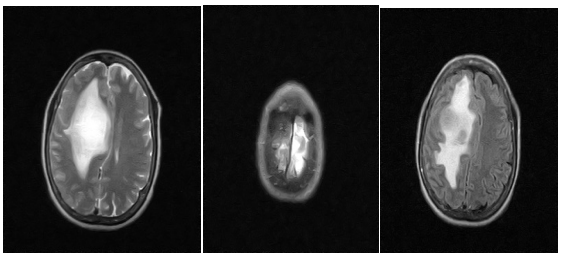

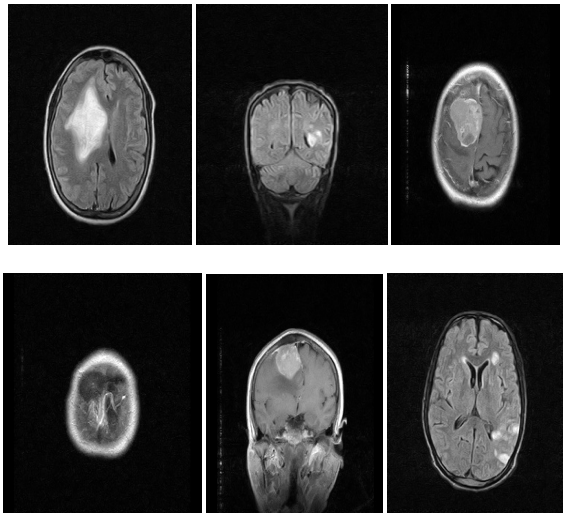

Figure 9. Clinical dataset used for validation studies

segmentation by an in-house expert rater. The level set evolution algorithm has been packaged in an easy to use product, integrated with an interface to manually initialize and clean-up the segmentation. The output of each segmentation is a binary image on the same voxel grid as the original MRI. We also applied the Encephalon Tumor segmentation to partition the tumor tissue further into its necrotic and enhancing parts. The tissues are further partitioned into various group of levels which are having same grades, this can be achieved by the fuzzy based clustering approach. Strengths of the proposed method include its simple interaction over a single slice and less sensitivity to the initialization its efficiency in terms of computation time, and robustness with respect to different and heterogeneous tumor types. Choosing the contrast enhanced T1 modality limits the application to the tumors that are enhanced with the contrast agent, excluding the edema/infiltration region around the tumor. For the targeted clinical application of radio surgery planning, using a single modality is an advantage due to the computational efficiency and ease of use. However, in a multi-modal scenario, it could be possible to design new transition functions adapted to a given modality and also optimize the parameters. The system, therefore, demonstrates high potential for practical clinical use, and may assist medical experts with tumor location, volumetric estimation, radio surgery, therapeutic planning and follow-up. Future aims include the improvement of the system's calculation loading, exploring the potential use of other MR modalities, and experimenting with the 3D image format.

5. Acknowledgment

The authors would like to thank Indian MRI Laboratory Radiation Center for providing the tumor dataset.

References

[1] S. Warfield, K. Zou, and W. Wells, "Simultaneous truth and perfor-
[2] mance level estimation (STAPLE): An algorithm for the

validation
[3] of image segmentation," IEEE Trans. Med Imag., vol. 23, no. 7, pp.
[4] 903-921, Jul. 2004.
[5] M.-R. Nazem-Zadeh, E. Davoodi-Bojd, and H. Soltanian-Zadeh,
[6] "Atlas based fiber bundle segmentation using principal diffusion
[7] directions and spherical harmonic coefficients," NeuroImage, vol. 54,
[8] pp. S146-S164, 2011.
[9] K. H. Zou, S. K. Warfield, A. Bharatha, C. M. C. Tempany, M. R. Kaus,
[10] S. J. Haker, W. M. Wells, F. A. Jolesz, and R. Kikinis, "Statistical vali-
[11] dation of image segmentation quality based on a spatial overlap index,"
[12] Acad. Radiol., vol. 11, no. 2, pp. 178-189, 2004.
[13] E. D. Angelini, O. Clatz, E. Mandonnet, E. Konukoglu, L. Capelle, and H. Duffau, "Glioma dynamics and computational models: A review of segmentation, registration, and in silico growth algorithms and their clinical applications," Curr. Med. Imag. Rev., vol. 3, no. 4, pp. 262-276, 2007.
[14] M. Prastawa, E. Bullitt, S. Ho, and G. Gerig, "A brain tumor segmentation framework based on outlier detection," Med. Image Anal., vol.8, no. 3, pp. 275-283, 2004.
[15] J. Liu, J. K. Udupa, D. Odhner, D. Hackney, and G. Moonis, "A system for brain tumor volume estimation via MR imaging and fuzzy connect-edness," Comput. Med. Imag. Graph., vol. 29, pp. 21-34, 2005..
[16] T. Biswas et al., "Stereotactic radiosurgery for glioblastoma: Retrospective analysis.," Radiation Oncology, vol. 4, no. 11, p. 11, 2009. A. Gooya, G. Biros, and C. Davatzikos, "Deformable registration of glioma images using em algorithm and diffusion reaction modeling,"
[17] IEEE Trans. Med. Imag., vol. 30, no. 2, pp. 375-390, Feb. 2011. B. Menze, K. V. Leemput, D. Lashkari, M.-A. Weber, N. Ayache, and P. Golland, "A generative model for brain tumor segmentation in multimodal images," Med. Image Comput. Comput. Assist. Intervent., vol. 13, pp. 151-159, Sep. 2010.
[18] T. F. Chan and L. Vese, "Active contours without edges," IEEE Trans.Image Process., vol. 10, no. 2, pp. 266-277, Feb. 2001.
[19] S. Ho, E. Bullitt, and G. Gerig, "Level-set evolution with region competition: Automatic 3-D segmentation of brain tumors," in Proc. ICPR,2002, vol. 1, p. 10532.
[20] Y. Boykov and M.-P. Jolly, "Interactive graph cuts for optimalboundary and region segmentation of objects in n-d images," in Proc.ICCV, 2001, pp. 105-112.
[21] L. Grady, "Random walks for image segmentation," in IEEE Trans.Pattern Anal. Mach. Intell., Nov. 2006, vol. 28, no. 11, pp. 1768-1783.
[22] C. Couprie, L. Grady, L. Najman, and H. Talbot, "Power watersheds: A new image segmentation framework extending graph cuts, random walker and optimal spanning forest," in ICCV, 2009, pp. 731-738.
[23] A. Sinop and L. Grady, "A seeded image segmentation framework Unifying graph cuts and random walker which yields a new algorithm," in ICCV, 2007, pp. 1-8. Criminisi, T. Sharp, and A. Blake, "GeoS: Geodesic image segmentation," in Comput. Vis. ECCV 2008, 2008, vol. 5302, pp. 99-112.
[24] X. Bai and G. Sapiro, "Geodesic matting: A framework for fast interactive image and video segmentation and matting," Int. J. Comput. Vis.,vol. 82, pp. 113-132, 2009.
[25] R. Szeliski, R. Zabih, D. Scharstein, O. Veksler, V. Kolmogorov, A Agarwala, M. Tappen, and C. Rother, "A comparative study of energy minimization methods for Markov random fields with smooth ness-based priors," IEEE Trans. Pattern Anal. Mach. Intell., vol. 30, pp. 1068-1080, 2008.
[26] V. Vezhnevets and V. Konouchine, "Growcut-interactive multi-label n-d image segmentation by cellular automata," presented at the
Graph icon, Novosibirsk Akademgorodok, Russia, 2005. Popovici and D. Popovici, "Cellular automata in image processing,"in Proc. 15th Int. Symp. Math. Theory Networks Syst., 2002, pp. 34-44.
[27] J. V. Neumann, Theory of self-reproducing automata, A. W. Burks,Ed . Champaign, IL: Univ. Illinois Press, 1966.
[28] N. Ganguly, B. K. Sikdar, A. Deutsch, G. Canright, and P. P. Chaudhuri, A survey on cellular automata Centre for high performance computing, Dresden Univ. Technol., Dresden, Germany, Tech. Rep., 2003. [23] J. Kari, "Theory of cellular automata: A survey," Theoretical Comput.Sci., vol. 334, no. 1-3, pp. 3-33, 2005.
[29] K. Kaneko, "Overview of coupled map lattices," Chaos, vol. 2, no. 3, pp. 279-282, 1992.
[30] D. N. Ostrov and R. Rucker, "Continuous-valued cellular automata for
[31] nonlinear wave equations," Complex Syst., vol. 10, pp. 91-119, 1996. [26] S. Wolfram, A New Kind of Science. Champaign, IL: Wolfram Media, 2002, ch. 4, p. 155.
A. Hamamci, G. Unal, N. Kucuk, and K. Engin,guru "Cellular automata segmentation of brain tumors on post contrast MR images," in MICCAI. New York: Springer, 2010, pp. 137-146.
B. Kauffmann and N. Pich, "Seeded ND medical image segmentation
[32] by cellular automaton on GPU," Int. J. Comput. Assist. Radiol. Surg., vol. 5, pp. 251-262, 2010.
[33] G. Hernandez and H. J. Herrmann, "Cellular automata for elementary image enhancement," Graphical Models Image Process., vol. 58, no. 1, pp. 82-89, 1996.
[34] C. Alvino, G. Unal, G. Slabaugh, B. Peny, and T. Fang, "Efficient segmentation based on eikonal and diffusion equations," Int. J. Comput. Math., vol. 84, pp. 1309-1324, Sept. 2007.
[35] P. Therasse, "Evaluation of response: New and standard criteria," Ann.Oncol., vol. 13, pp. 127-129, 2002.
[36] L. S. Chin, L. Ma, and S. Dibiase, "Radiation necrosis following gamma knife surgery: A case-controlled comparison of treatment parameters and long-term clinical follow up," J. Neurosurg., vol. 94, pp. 899-904, 2001.
A. P. Dempster, N. M. Laird, and D. B. Rubin, "Maximum likelihood
[37] from incomplete data via the EM algorithm," J. R. Stat. Soc., Series B, vol. 39, no. 1, pp. 1-38, 1977.
[38] N. Otsu, "A threshold selection method from gray level histograms,"
[39] IEEE Trans. Syst., Man Cybern., vol. 9, no. 1, pp. 62-66, Mar. 1979. [35] M. Prastawa, E. Bullitt, and G. Gerig, "Synthetic ground truth for validation of brain tumor MRI segmentation," in MICCAI. New York: Springer, 2005, pp. 26-33.